CHIN. PHYS. LETT. Vol. 36, No. 5 (2019) 057102

Negative Longitudinal Magnetoresistance in the *c*-Axis Resistivity of Cd *

Xin-Min Wang(王欣敏)[1,2], Ling-Xiao Zhao(赵凌霄)[1], Jing Li(李婧)[1,2], Mo-Ran Gao(高默然)[1,2], Wen-Liang Zhu(朱文亮)[1,2], Chao-Yang Ma(麻朝阳)[1], Yi-Yan Wang(王义炎)[1], Shuai Zhang(张帅)[1], Zhi-An Ren(任治安)[1,2,3], Gen-Fu Chen(陈根富)[1,2,3]**

[1]*Institute of Physics and Beijing National Laboratory for Condensed Matter Physics, Chinese Academy of Sciences, Beijing 100190*

[2]*School of Physical Sciences, University of Chinese Academy of Sciences, Beijing 100049*

[3]*Songshan Lake Materials Laboratory, Dongguan 523808*

(Received 28 January 2019)

We report a systematic study on magnetotransport properties of the single crystal of cadmium (Cd). When the applied magnetic field B is perpendicular to the current I, the resistivities for both directions ($I \parallel a$, $I \parallel c$) show field induced metal-to-insulator-like transitions. The isothermal magnetoresistance (MR) at low temperatures increases approximately as the square of the magnetic field without any sign of saturation, and reaches up to 1140000% and 58000% at $T = 2\,K$ and $B = 9\,T$ for $I \parallel a$ and $I \parallel c$, respectively. As the magnetic field rotates to parallel to the current, no sign of negative MR is observed for $I \parallel a$, while an obvious negative MR appears up to -70% at $2\,K$ and $9\,T$ for the current flowing along the c-axis, and the negative longitudinal MR shows a strong dependence of the electrode position on the single crystal. These results suggest that the negative longitudinal MR is caused by the dislocations formed in the process of crystal growing along the c-axis. Further studies are needed to clarify this point.

PACS: 71.55.Ak, 71.30.+h, 75.47.−m, 81.10.Bk

DOI: 10.1088/0256-307X/36/5/057102

Topological semimetals (TSMs) such as Dirac and Weyl semimetals have recently attracted a great deal of attention due to their exotic transport properties.[1−10] The negative magnetoresistance (MR) is a consequence of chiral anomaly, which is related to the nonconservation of the number of quasiparticles with a given chirality.[11] It has been reported that this extraordinary property of negative MR exists in the case that the magnetic field is parallel to the electric field,[7,12−14] as observed in Dirac semimetal Cd_3As_2[2,3] and Na_3Bi,[7] Weyl semimetal TaAs.[5] However, the observation of negative MR in the transport measurements is not the fingerprint of the Weyl metallic state. The negative MR could also be caused by the size effect[15−19] or extreme quantum limit effect.[20,21] In thin bismuth nanowires, the negative MR is caused by the reduced boundary scattering, which is because a higher magnetic field can squeeze electrons off the walls as the electron cyclotron radius becomes comparable to the wires radius.[15] In the extreme quantum limit, electrons can be confined to the lowest Landau level, and then the reversal of electron momentum under the magnetic field can be suppressed. Thus, the negative MR appears as the consequence of reduced backward scattering.[20] In addition, crystal defects, particularly dislocations produced during crystal growth, and the current-jetting effect, caused by the geometry of the samples can also induce the negative MR.[22,23]

Recently, both theoretical and experimental investigations indicated that the simple chemical element gray arsenic (gray-As) is a topological insulator (TI),[24,25] which exhibits many exotic transport behaviors, such as extremely large MR, ultrahigh carrier mobility, nontrivial π Berry phase and negative longitudinal MR. Similar to gray-As, theoretical calculation also suggested that the simple chemical element cadmium (Cd) is a TI with the spin-orbit coupling (SOC), and/or a high symmetry line semi-metal without SOC.[26] In this work, we prepare the high quality single crystals of Cd, which grow along the *a*-axis and *c*-axis directions, respectively. We perform the anisotropic MR and the *c*-axis transport property studies for the first time, and find that Cd has field-induced metal-to-insulator-like transitions, and large nonsaturating MR for both the directions ($I \parallel a$, $I \parallel c$), as observed in other TSMs. Notably, in the presence of parallel magnetic and electric fields, a weak antilocalization (WAL)-like effect and a pronounced negative longitudinal MR are observed in *c*-axis transport measurements. Furthermore, this negative longitudinal MR strongly depends upon the electrode placement on the crystal. We discuss whether or not this negative longitudinal MR in the *c*-axis is associated with the dislocations formed in the process of crystal growing along the *c*-axis.

In our experiment, high quality single crystals of Cd were grown by the vapor-phase transport method.

*Supported by the National Key Research Program of China under Grant Nos 2016YFA0401000 and 2016YFA0300604, the National Basic Research Program of China under Grant No 2015CB921303, the Strategic Priority Research Program (B) of Chinese Academy of Sciences under Grant No XDB07020100, and the National Natural Science Foundation of China under Grant No 11874417.

**Corresponding author. Email: gfchen@iphy.ac.cn

© 2019 Chinese Physical Society and IOP Publishing Ltd

The quartz tube with appropriate amounts of starting material Cd (99.9997%) was evacuated and kept at the growth temperature for two weeks in a two-zone furnace. Shiny plate-like crystals were produced in a temperature gradient of 300℃–200℃. The obtained crystals were characterized by x-ray diffraction (XRD) using PANalytical diffractometer (Cu $K_{\alpha 1}$ radiation, $\lambda = 1.54051$ Å) at room temperature. The magnetotransport measurements were performed with the four-probe method in a Quantum Design PPMS. To achieve a uniform current distribution and to avoid the current-jetting effect, slender single crystals were chosen for transport property experiments and the current leads were prepared by painting silver paste over the whole front and end surfaces of the specimens.

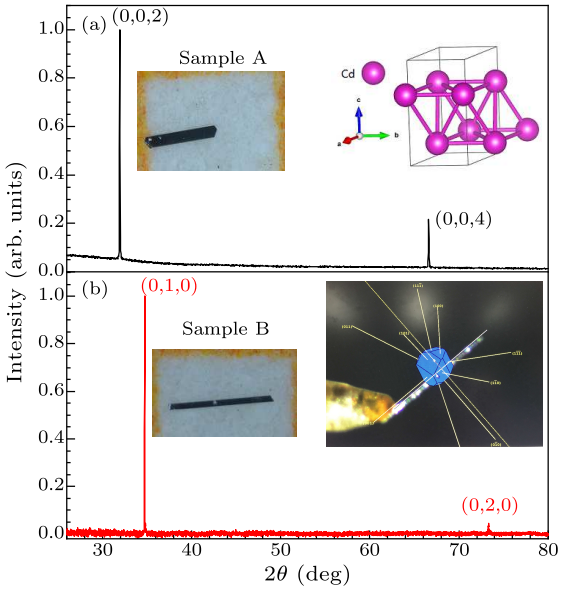

Fig. 1. (Color online) XRD patterns of single crystals of Cd. The insets on the left depict two typical photographs of obtained Cd crystals. The right inset in (a) shows the crystal structure of Cd. The picture in the right inset of in (b) shows the single-crystal diffraction at room temperature for sample B.

Cd crystallizes in a hexagonal layered structure stacking along the c-axis with space group $P63mmc$ (No. 194), and the crystal structure is illustrated in the right inset of Fig. 1(a). The plate-like crystals were found to grow in two different types, with one type growing along the a-axis and the other along the c-axis. As shown in Figs. 1(a) and 1(b), the XRD patterns of two selected single crystals (labeled as samples A and B) could be well indexed as $(00l)$ and $(0k0)$ reflections, respectively.

Systematic magnetotransport properties were performed on the two types of single crystals. Figures 2(a) and 2(b) display the temperature dependence of the resistivity $\rho_{\rm ab}$ ($I \parallel a$) and ρ_c ($I \parallel c$) under different fields. The measurement configurations are shown in the insets. Here $\rho_{\rm ab}$ shows a metallic behavior in zero magnetic field with the residual resistivity ratio (RRR $= \rho(300\,{\rm K})/\rho(2\,{\rm K})$) up to 5500, indicating that the grown single crystal is of high quality. It is obvious that ρ_c is one order of magnitude larger than that of $\rho_{\rm ab}$. This phenomenon is also reported in many layered materials, and originates from the anisotropy of carrier mobility.[27] When the magnetic field is applied perpendicular to the flowing current ($B \perp I$), the resistivities for both directions ($I \parallel a$ and $I \parallel c$) show a magnetic field induced metal-to-insulator-like transition and a resistivity plateau at low temperatures. The transition temperature increases with the magnetic field strength. These exotic behaviors have also been observed in the recently discovered semimetals such as WTe_2,[1] TaAs,[5] as well as gray-As,[24] but the intrinsic origin is still unclear.

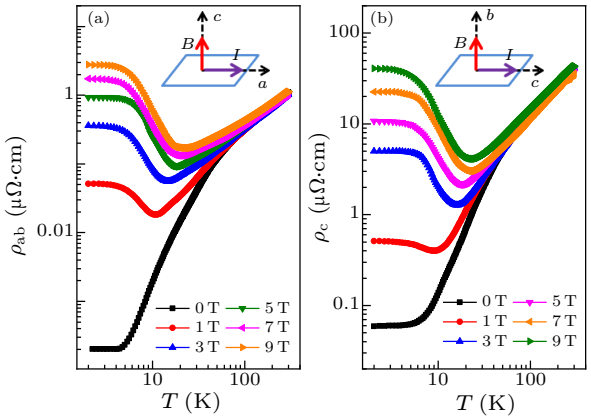

Fig. 2. The temperature dependence of (a) resistivity ρ_{ab} and (b) ρ_c under different fields with $B \perp I$ on a log-log scale.

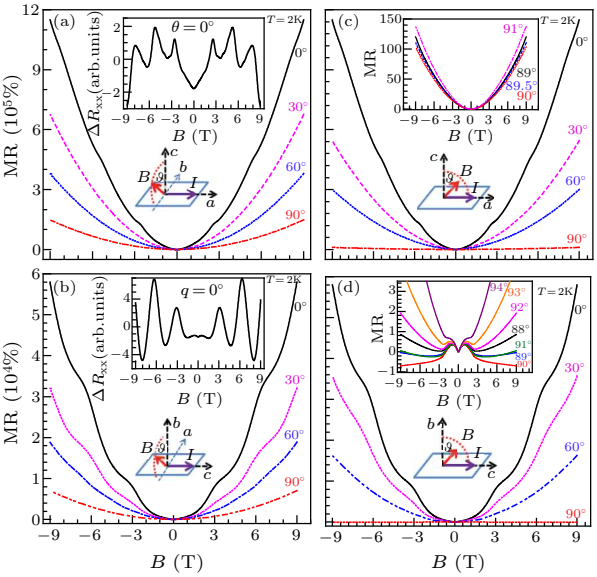

Fig. 3. The magnetic field dependence of MR at 2 K with the magnetic field rotated in the plane always perpendicular to the current for both directions ((a) $I \parallel a$, (b) $I \parallel c$), where the insets show the oscillations terms ΔR_{xx} by subtracting the polynomial background from MR. The magnetic field dependence of MR at 2 K by tilting the field from perpendicular to parallel to the current for both directions ((c) $I \parallel a$, (d) $I \parallel c$), where the insets show the measurement configurations.

Figures 3(a) and 3(b) show the magnetic

field dependence of MR (defined as $(\rho_{xx}(B,T) - \rho_{xx}(0,T))/\rho_{xx}(0,T)$) at 2 K with the magnetic field rotated in the plane always perpendicular to the current for both the samples, where θ is defined as the angle between the field direction and the normal vector of the sample surface. For both the measurement configurations ($I \parallel a$ and $I \parallel c$), MR decreases monotonically with increasing θ. At $\theta = 0°$, large positive MR values up to 1140000% and 58000% were obtained at 9 T for $I \parallel a$ and $I \parallel c$, respectively. The MR for the field always perpendicular to current shows a near parabolic behavior up to 9 T without saturation, which can be related to the compensation mechanism in Cd,[28] as reported in WTe_2[1] and gray-As.[24]

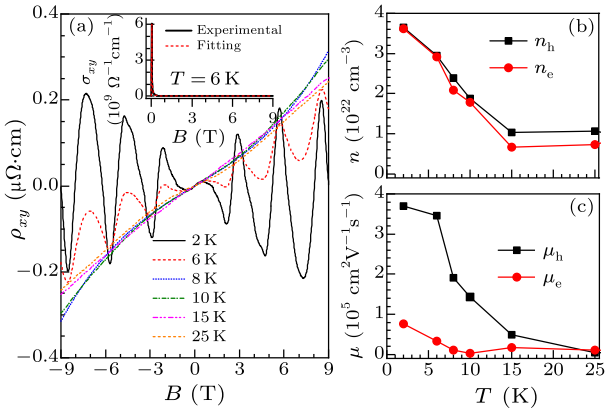

Fig. 4. (a) The magnetic field dependence of Hall resistivity ρ_{xy} at various temperatures from 2 K to 25 K. The inset shows the experimental data of Hall conductivity at 6 K and the fitted curve. (b) The temperature dependence of carrier densities. (c) The temperature dependence of carrier mobilities deduced by the two-carrier model.

To further confirm the compensation effect, we performed the Hall-effect measurements at various temperatures with the current along the a-axis direction, as shown in Fig. 4. The nonlinear behavior of the Hall resistivity implies that Cd is a multiband system. We try to fit the Hall resistivity using the semi-classical two-band model, in which the Hall conductivity σ_{xy} can be expressed as[8]

$$\sigma_{xy} = \left(\frac{n_{\rm h}\mu_{\rm h}^2}{1+(\mu_{\rm h}B)^2} - \frac{n_{\rm e}\mu_{\rm e}^2}{1+(\mu_{\rm e}B)^2}\right)eB, \qquad (1)$$

where $n_{\rm e}$ ($n_{\rm h}$) and $\mu_{\rm e}$ ($\mu_{\rm h}$) denote the carrier density and mobility of electron (hole), respectively. The obtained temperature dependence of n and μ are shown in Figs. 4(b) and 4(c), respectively. The mobilities and densities of the two types of carriers decrease with increasing temperature. It is clearly seen that at low temperatures ($T < 15$ K), the mobility of holes is larger than that of electrons by one order of magnitude, and the very slight difference between $n_{\rm e}$ and $n_{\rm h}$ demonstrates clearly that two kinds of carriers are of perfect compensation, resulting in the large unsaturated MR.[1,24]

Interestingly, clear oscillations are observed in MR and Hall resistivity with a period of B rather than $1/B$, as reported in the previous works.[29,30] The B-periodic oscillations were commonly observed in nanoscale materials, which can be ascribed to the size effect as the mean free path is comparable to, or larger than, the thickness of the sample.[31] In such a large single crystal of Cd, the oscillations were considered to be associated with the lens-shaped pocket of electrons in the third Brillouin zone in which the electrons have a large millimeter-scale mean free path.[30]

The MR at 2 K by tilting the field from perpendicular to parallel to current directions (current flowing along the a and c axes) are presented in Figs. 3(c) and 3(d), respectively. For $I \parallel a$, MR decreases dramatically with increasing θ but is still 8000% at 9 T at $\theta = 90°$. The nonzero value is caused by the slight asymmetry of the two electrodes.

Surprisingly, as shown in Fig. 3(d), the MR for $I \parallel c$ decreases monotonically with the increase of θ, and a negative MR with a value of about -70% was observed at $B = 9$ T and $\theta = 90°$ ($B \parallel I$). The negative MR, as reported in Weyl semimetal TaAs and topological semimetal gray-As, is more sensitive to the angle between the magnetic field and the current direction.[5,24] To further confirm the observed longitudinal negative MR, we also characterized the field dependence of MR at different angles around $\theta = 90°$ with the interval of every 1°, as shown in the inset of Fig. 3(d). The negative MR only presents with tilting the field direction 4° away from the current, and most obviously when $B \parallel I$. We found that the MR increases sharply in low magnetic field range ($0\,{\rm T} < |B| < 1\,{\rm T}$) and drops dramatically in the range of $1\,{\rm T} < |B| < 3\,{\rm T}$ and then tends to saturation at higher fields. Usually, a sharp MR dip around zero magnetic field is associated with the WAL effect, which is observed commonly in graphene and TIs, in which Dirac fermions dominate the magnetoelectric transport.[32,33] The negative longitudinal MR and WAL-like features were found to be very sensitive to the temperature variations, as shown in Fig. 5(a), which would disappear rapidly when the sample was warmed up to 15 K, similar to that of gray-As.[24]

To further understand the observed negative longitudinal MR, we also fit the data using a semiclassical formula[24] in the magnetic field $-2.5\,{\rm T} \leq B \leq 2.5\,{\rm T}$,

$$\sigma_B = (1 + C_{\rm W}B^2)\sigma_{\rm WAL} + \sigma_{\rm N}, \qquad (2)$$

with

$$\sigma_{\rm WAL} = \sigma_0 + a\sqrt{B}, \qquad (3)$$

$$\sigma_{\rm N}^{-1} = \rho_0 + AB^2, \qquad (4)$$

where σ_0 is the zero field conductivity, and $C_{\rm W}$ is a positive parameter which originates from the topological $E \cdot B$. Such a topological term will generate chiral current in the nonorthogonal magnetic and electric fields. Here $\sigma_{\rm WAL}$ and $\sigma_{\rm N}$ are those from WAL effect and conventional nonlinear band contributions around the Fermi level, respectively. Figure 5(b) shows the experimental data (open circles) and

the fitting curves (red dashed lines) at various temperatures and the fittings show excellent agreement between the experimental data and theoretical curves with the parameters of $\sigma_0 = 7.747 \times 10^6\,\Omega^{-1}\mathrm{cm}^{-1}$, $a = -5.06 \times 10^7\,\Omega^{-1}\mathrm{m}^{-1}\mathrm{T}^{-0.5}$, $C_\mathrm{W} = 0.314\mathrm{T}^{-2}$, $A = 3.405 \times 10^{-7}\,\Omega\mathrm{cm}\mathrm{T}^{-2}$ and $\rho_0 = 1.291 \times 10^{-7}\,\Omega\mathrm{cm}$ at $T = 2\,\mathrm{K}$. It seems to suggest that Cd has a signature of Dirac fermions characters as detected in other topological semimetals. Further angle-resolved photoemission spectroscopy (ARPES) measurements are necessary to clarify this issue.

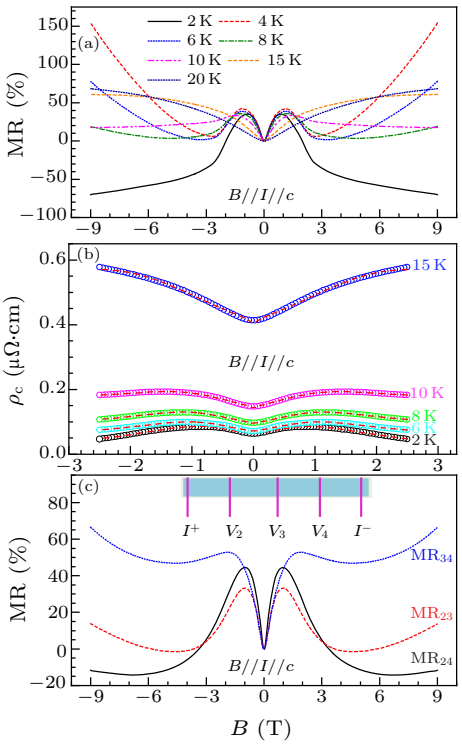

Fig. 5. (a) The magnetic field dependence of the negative MR at various temperatures for $B \parallel I \parallel c$ measurement configuration. (b) The field dependence of negative MR (open circles) and the fit data (dotted line) at various temperatures for $B \parallel I \parallel c$. (c) The longitudinal MR was measured on the crystal growing along the c-axis with different electrode placements.

It should be noted that the negative longitudinal MR only appears in the c-axis, while no sign of negative longitudinal MR was observed as the current flowing along the a-axis. In contrast, the negative longitudinal MR observed in gray-As is not directional.[24] Considering the layered crystal structure stacking along the c-axis, the dislocations formed in the process of crystal growing along the c-axis may also lead to the emergence of negative MR, as reported in deformed InSb.[23] Recently, it was predicted that dislocations could also cause the negative MR in Dirac semimetals,[34,35] in which fermionic quasiparticles may appear from vacuum under an external electric field and result in a nonzero axial (chiral) charge in the vicinity of the dislocation. To clarify the origin of the observed negative longitudinal MR, an addition electrode was positioned on the single crystal growing along the c-axis. The magnetic field dependence of longitudinal MR_{23} (detected between V_2 and V_3), MR_{34} (detected between V_3 and V_4) and MR_{24} (detected between V_2 and V_4) are shown in Fig. 5(c). Obviously, the longitudinal MRs tested between different electrodes show various field-dependence behaviors above 1 T, suggesting that the observed negative MR may not be an intrinsic property of the material but a secondary effect dependent upon the quality of the sample. Further studies are necessary to clarify this point.

In summary, we have successfully grown high quality single crystals of Cd and have studied their magnetotransport properties in detail. The single crystals of Cd show metallic behavior at zero field. Upon application of magnetic field, the temperature dependences of resistivity for both $I \parallel a$ and $I \parallel c$ directions show field-induced metal-to-insulator-like transitions and saturation at low temperatures. With the magnetic field applied parallel to the flowing current, no signal of negative MR can be observed at 2 K for $I \parallel a$. However, with changing the current flowing along the c-axis, an obvious negative MR is detected with a sharp MR dip around zero magnetic field, and the negative MR in the c-axis strongly depends on the placements of electrodes on the crystal. Based on these experimental results, we speculate that this negative longitudinal MR in the c-axis is associated with the dislocations formed in the process of crystal growing along the c-axis.

References

[1] Ali M N, Xiong J, Flynn S, Tao J, Gibson Q D, Schoop L M, Liang T, Haldolaarachchige N, Hirschberger M, Ong N P and Cava R J 2014 *Nature* **514** 205
[2] Liang T, Gibson Q, Ali M N, Liu M H, Cava R J and Ong N P 2015 *Nat. Mater.* **14** 280
[3] Li C Z, Wang L X, Liu H W, Wang J, Liao Z M and Yu D P 2015 *Nat. Commun.* **6** 10137
[4] Weng H M, Fang C, Fang Z, Bernevig B A and Dai X 2015 *Phys. Rev. X* **5** 011029
[5] Huang X C, Zhao L X, Long Y J, Wang P P, Chen D, Yang Z H, Liang H, Xue M Q, Weng H M, Fang Z, Dai X and Chen G F 2015 *Phys. Rev. X* **5** 031023
[6] Shekhar C, Nayak A K, Sun Y, Schmidt M, Nicklas M, Leermakers I, Zeitler U, Skourski Y, Wosnitza J, Liu Z K, Chen Y L, Schnelle W, Borrmann H, Grin Y, Felser C and Yan B H 2015 *Nat. Phys.* **11** 645
[7] Xiong J, Kushwaha S K, Liang T, Krizan J W, Hirschberger M, Wang W D, Cava R J and Ong N P 2015 *Science* **350** 413
[8] Chen D, Zhao L X, He J B, Liang H, Zhang S, Li C H, Shan L, Wang S C, Ren Z A, Ren C and Chen G F 2016 *Phys. Rev. B* **94** 174411
[9] Arnold F, Shekhar C, Wu S C, Sun Y, dos Reis R D, Kumar N, Naumann M, Ajeesh M O, Schmidt M, Grushin A G, Bardarson J H, Baenitz M, Sokolov D, Borrmann H, Nicklas M, Felser C, Hassinger E and Yan B H 2016 *Nat. Commun.* **7** 11615
[10] He J B, Chen D, Zhu W L, Zhang S, Zhao L X, Ren Z A and Chen G F 2017 *Phys. Rev. B* **95** 195165
[11] Li C H, Long Y J, Zhao L X, Shan L, Ren Z A, Zhao J Z, Weng H M, Dai X, Fang Z, Ren C and Chen G F 2017 *Phys. Rev. B* **95** 125417

[12] Son D T and Spivak B Z 2013 *Phys. Rev. B* **88** 104412
[13] Burkov A A 2015 *Phys. Rev. B* **91** 245157
[14] Zhang C L, Xu S Y, Belopolski I, Yuan Z J, Lin Z Q, Tong B B, Bian G, Alidoust N, Lee C C, Huang S M, Chang T R, Chang G Q, Hsu C H, Jeng H T, Neupane M, Sanchez D S, Zheng H, Wang J F, Lin H, Zhang C, Lu H Z, Shen S Q, Neupert T, Hasan M Z and Jia S 2016 *Nat. Commun.* **7** 10735
[15] Gurvitch M 1980 *Jour. Low-Temp. Phys.* **38** 777
[16] Thornton T J, Roukes M L, Scherer A and Vandegaag B P 1989 *Phys. Rev. Lett.* **63** 2128
[17] Heremans J, Thrush C M, Zhang Z, Sun X, Dresselhaus M S, Ying J Y and Morelli D T 1998 *Phys. Rev. B* **58** R10091
[18] Yang F Y, Liu K, Chien C L and Searson P C 1999 *Phys. Rev. Lett.* **82** 3328
[19] Heremans J, Thrush C M, Lin Y M, Cronin S B and Dresselhaus M S 2001 *Phys. Rev. B* **63** 085406
[20] Argyres P N and Adams E N 1956 *Phys. Rev.* **104** 900
[21] Mansfield R and Azhdarov G 1978 *Phys. Stat. Sol. (b)* **87** 163
[22] Hu J S, Rosenbaum T F and Betts J B 2005 *Phys. Rev. Lett.* **95** 186603
[23] Broom R F 1958 *Proc. Phys. Soc.* **71** 470
[24] Zhao L X, Xu Q N, Wang X M, He J B, Li J, Yang H X, Long Y J, Chen D, Liang H, Li C H, Xue M Q, Li J Q, Ren Z A, Lu L, Weng H M, Fang Z, Dai X and Chen G F 2017 *Phys. Rev. B* **95** 115119
[25] Zhang P, Ma J Z, Ishida Y, Zhao L X, Xu Q N, Lv B Q, Yaji K, Chen G F, Weng H M, Dai X, Fang Z, Chen X Q, Fu L, Qian T, Ding H and Shin S 2017 *Phys. Rev. Lett.* **118** 046802
[26] Zhang T T, Jiang Y, Song Z D, Huang H, He Y Q, Fang Z, Weng H M and Fang C 2019 *Nature* **566** 475
[27] Matsubara K, Sugihara K and Tsuzuku T 1990 *Phys. Rev. B* **41** 969
[28] Katyal O P and Gerritsen A N 1969 *Phys. Rev.* **178** 1037
[29] Zebouni N H, Hamburg R E and Mackey H J 1963 *Phys. Rev. Lett.* **11** 260
[30] Mackey H J, Sybert J R and Fielder J T 1967 *Phys. Rev.* **157** 578
[31] Sondheimer E H 1950 *Phys. Rev.* **80** 401
[32] Liu M H, Zhang J S, Chang C Z, Zhang Z C, Feng X, Li K, He K, Wang L L, Chen X, Dai X, Fang Z, Xue Q K, Ma X C and Wang Y Y 2012 *Phys. Rev. Lett.* **108** 036805
[33] Ishiwata S, Shiomi Y, Lee J S, Bahramy M S, Suzuki T, Uchida M, Arita R, Taguchi Y and Tokura Y 2013 *Nat. Mater.* **12** 512
[34] Zubkov M A 2015 *Ann. Phys.* **360** 655
[35] Chernodub M N and Zubkov M A 2017 *Phys. Rev. B* **95** 115410